

**Gamow-Teller decay of the  $T = 1$  nucleus  $^{46}\text{Cr}$** 

T. K. Onishi,<sup>1</sup> A. Gelberg,<sup>2,3</sup> H. Sakurai,<sup>1</sup> K. Yoneda,<sup>3</sup> N. Aoi,<sup>3</sup> N. Imai,<sup>1</sup> H. Baba,<sup>4</sup> P. von Brentano,<sup>2</sup> N. Fukuda,<sup>3</sup> Y. Ichikawa,<sup>1</sup> M. Ishihara,<sup>3</sup> H. Iwasaki,<sup>1</sup> D. Kameda,<sup>5</sup> T. Kishida,<sup>3</sup> A. F. Lisetskiy,<sup>6</sup> H. J. Ong,<sup>1</sup> M. Osada,<sup>1</sup> T. Otsuka,<sup>1</sup> M. K. Suzuki,<sup>1</sup> K. Ue,<sup>1</sup> Y. Utsuno,<sup>7</sup> and H. Watanabe<sup>3</sup>

<sup>1</sup>*Department of Physics, University of Tokyo, Hongo 7-3-1, Bunkyo-ku, 113-0033 Tokyo, Japan*

<sup>2</sup>*Institut für Kernphysik der Universität zu Köln, D-50937 Köln, Germany*

<sup>3</sup>*Institute of Physical and Chemical Research (RIKEN), Hirosawa 2-1, Wako-shi, 351-0198 Japan*

<sup>4</sup>*Department of Physics, Rikkyo University, Nishi-Ikebukuro 3-34-1, Toshima, Tokyo, Japan*

<sup>5</sup>*Department of Physics, Tokyo Institute of Technology, Ookayama 2-12-1, Meguro, Tokyo, Japan*

<sup>6</sup>*Michigan State University, Cyclotron, East Lansing, Michigan 48824, USA*

<sup>7</sup>*Japan Atomic Energy Research Institute, Tokai-mura, 319-1195 Japan*

(Received 23 March 2005; published 16 August 2005)

The Gamow-Teller  $\beta$  decay of  $^{46}\text{Cr}$  to the  $N = Z$  odd-odd nucleus  $^{46}\text{V}$  has been observed for the first time.  $^{46}\text{Cr}$  was produced by the fragmentation of a  $^{50}\text{Cr}$  primary beam at 80 MeV/nucleon. By means of  $\beta$ - $\gamma$  coincidence measurements, a  $\gamma$ -ray peak at 993 keV corresponding to the decay of the  $1^+$  state in  $^{46}\text{V}$  was observed. The branching ratio of the Gamow-Teller decay to this state was found to be  $b_{\text{GT}} = 0.216 \pm 0.050$ . The half-life of  $^{46}\text{Cr}$  was measured to be  $T_{1/2} = 240 \pm 140$  ms. The transition strength was determined to be  $B(\text{GT}) = 0.64 \pm 0.20$ . This result was compared with theoretical values calculated with the shell model and the phenomenological quasideuteron model.

DOI: [10.1103/PhysRevC.72.024308](https://doi.org/10.1103/PhysRevC.72.024308)

PACS number(s): 23.60.+e, 23.40.Hc, 25.70.Mn

**I. INTRODUCTION**

$\beta$  decay is a major source of information on nuclear structure. In particular, Gamow-Teller (GT) transitions generated by the spin-isospin  $\sigma t_{\pm}$  operator are extremely sensitive to two-body interactions. Experimental data, e.g., excitation energies and transition matrix elements, provide useful information on these interactions, a good understanding of which is required for a correct description of nuclear properties.

The  $\beta$  decay of  $^{46}\text{Cr}$  is of particular interest since the  $^{46}\text{Cr}$  nucleus is expected to have a strong GT decay branch, as a nucleus with  $|N - Z| = 2$  and mass number  $A = 4n + 2$  (for  $n$  an integer). Such  $T = 1$  nuclei decay to the  $T = 0$  and  $I^{\pi} = 1^+$  states of daughter nuclei via the so-called favored-allowed GT transitions [1], which are characterized by small  $ft$  values. One example is  $^6\text{He}$ , which decays to the ground state (g.s.) of  $^6\text{Li}$  with  $ft = 813$  ( $\log ft = 2.91$ ). For light nuclei, Wigner SU(4) symmetry [2] helps explain the small  $ft$  values of nuclei with  $|N - Z| = 2$  and  $A = 4n + 2$ . With increasing nuclear mass, the SU(4) symmetry is increasingly broken due to relatively large  $LS$  coupling or deformation effects [1]. Nevertheless, the favored-allowed character of the GT transitions survives at least up to the  $pf$  shell.

The favored-allowed GT transitions of nuclei with  $|N - Z| = 2$  and  $A = 4n + 2$  have been observed up to  $^{58}\text{Zn}$ , with the exception only of the decay of  $^{46}\text{Cr}$ . The decay of  $^{46}\text{Cr}$  was first investigated by Zioni *et al.* [3], who used the  $^{32}\text{S}(^{16}\text{O}, 2n)$  reaction to produce  $^{46}\text{Cr}$ . Activity with  $T_{1/2} = 260 \pm 60$  ms was ascribed to the Fermi decay of  $^{46}\text{Cr}$  to the  $I^{\pi} = 0^+$  g.s. of  $^{46}\text{V}$ . No delayed  $\gamma$  transitions associated with the same half-life were observed.

In recent years, an excited  $1^+$  state at  $993 \pm 0.4$  keV has been identified for  $^{46}\text{V}$  [4] by measuring the angular distribution and polarization of 993 keV  $\gamma$  rays. This spin-parity assignment has been independently confirmed [5,6]. The large

$B(M1)$  value of the transition to the  $I^{\pi} = 0^+$ ,  $T = 1$  g.s. indicates its isovector character. Therefore, the  $1^+$  state at 993 keV should have  $T = 0$ . Thus, one would expect a GT decay of  $^{46}\text{Cr}$  to the first  $1^+$  excited state of  $^{46}\text{V}$ .

The GT decay study of  $^{46}\text{Cr}$  gives unique information on nuclear structure in the midregion of the  $pf$  shell, where possible deformation may affect GT decay. It is expected that the  $1^+$  states of a spherical potential are fragmented by the coupling to collective degrees of freedom. Shell model calculations [4], suggest there should be at least two excited  $1^+$ ,  $T = 0$  states in the 0–3 MeV energy range. At the same time, the associated GT strengths should also be fragmented. Besides the shell model, a phenomenological model, the quasideuteron (QD) model [7], is also useful for revealing the effects of deformation on GT decay, where  $T = 1$  and  $T = 0$  pairs of nucleons are simply coupled to a deformed  $N = Z$  core.

The main aim of this work is to define the GT decay of  $^{46}\text{Cr}$  to the first excited  $1^+$  state of  $^{46}\text{V}$  and to other  $1^+$  states if they exist, and to compare results with shell model and phenomenological calculations. In the following, we first describe the experimental setup and procedure in Sec. II. In Sec. III, we describe the method of data analysis and present the experimental results, including the observed 993 keV peak, the branching ratio to the  $1^+$  state, and the half-life of  $^{46}\text{Cr}$ . Based on these results, we determine the GT transition strength. In Sec. IV, we compare the results with shell model and phenomenological calculations.

**II. EXPERIMENTAL SETUP**

This study was performed at RIKEN Projectile Fragment Separator (RIPS) [8] in the RIKEN accelerator research facility. A  $^{46}\text{Cr}$  beam was produced by the projectile

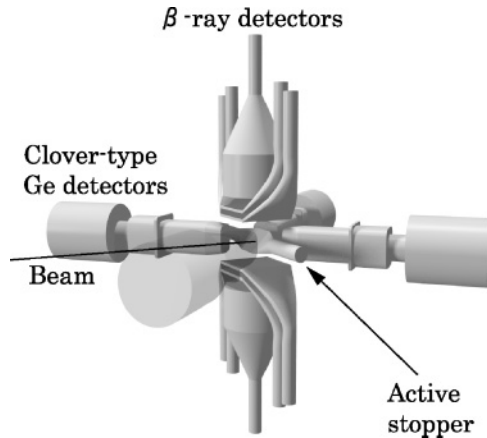


FIG. 1. Experimental setup for the  $\beta$ - $\gamma$  coincidence measurement.

fragmentation reaction of  $^{50}\text{Cr}$ , and the nuclei were implanted into an active stopper made of a plastic scintillator.  $\beta$  and  $\gamma$  rays from the implanted nuclei were observed to deduce  $T_{1/2}$  and the branching ratios. Figure 1 shows a schematic view of the detectors for the  $\beta$  and  $\gamma$  rays. The  $\beta$  rays were detected by plastic scintillators, while the  $\gamma$  rays were detected by Ge detectors. In the following, details of the detector setup and experimental techniques are described.

Radioactive ions were produced by projectile fragmentation of an 80 MeV/nucleon  $^{50}\text{Cr}$  primary beam with a beam intensity of 5 pA. We used a primary beam of  $^{50}\text{Cr}$  enriched to 60%, which has a natural abundance of only 4.3%, to obtain a  $^{46}\text{Cr}$  beam of reasonably good purity. The production target was  $^9\text{Be}$  with a thickness of 139 mg/cm<sup>2</sup>. The thickness of the production target was chosen so as to maximize the yield of  $^{46}\text{Cr}$ , using a semiempirical yield estimation by the INTENSITY code [9]. The reaction fragments were collected and analyzed by RIPS in an achromatic mode. An aluminum wedge degrader with a mean thickness of 116 mg/cm<sup>2</sup> was placed at the momentum dispersive focus (F1) for isotope separation. The secondary  $^{46}\text{Cr}$  beam had an intensity of about 40 particles per second and an isotope purity of 0.1% at the first achromatic focal plane of RIPS (F2). The beam was pulsed for measuring the half-life of  $^{46}\text{Cr}$ . The durations of the beam-on and beam-off periods were chosen to be 500 and 790 ms, respectively, to match the half-life of  $^{46}\text{Cr}$  [3].

The radioactive ions were implanted into the active stopper located at the final focal plane (F3) of RIPS. The number of implanted ions was counted using the stopper itself. For the active stopper, we used a 2-mm-thick plastic scintillation detector with an area of 100 × 100 mm<sup>2</sup>. The active stopper was tilted at an angle of 45° to the horizontal plane to decrease disturbance of the  $\beta$ -ray detection. In front of the stopper, we placed an 18-mm- $\phi$  stainless steel collimator so that nuclei were implanted only in the central region of the stopper. In addition to counting the total number of implanted ions, determining the ratio of implanted  $^{46}\text{Cr}$  to the total number of implanted ions was also necessary to obtain the number of implanted  $^{46}\text{Cr}$ . To obtain the ratio, each of the incoming nuclei were identified by time-of-flight (TOF) information in a separate run. The TOF was measured with a RF signal and a

0.1-mm-thick plastic scintillation detector, located at F2. In a further run, aimed at checking the purity of  $^{46}\text{Cr}$  in the range of the TOF of  $^{46}\text{Cr}$ , we identified each of the incoming nuclei by  $\Delta E$ -TOF information using a 0.35-mm-thick silicon detector, placed at F2 to measure  $\Delta E$ . When using this silicon detector, the  $^{46}\text{Cr}$  nuclei were stopped before the stopper because the range of  $^{46}\text{Cr}$  was rather short. To monitor the transmission efficiency between F2 and the stopper, the beam profile at the collimator was measured by two PPACs (F3PPACs) located upstream of the collimator at 92 and 122 cm, respectively.

Four clover-type Ge detectors (Ortec) were used to detect  $\gamma$  rays from the  $\beta$  decay of  $^{46}\text{Cr}$ . The high energy resolution of these detectors enabled us to separate  $\gamma$  rays originating from various sources and to attain a good sensitivity to low-intensity  $\gamma$  rays. Each Ge detector was located at 12 cm from the stopper. A  $^{152}\text{Eu}$  standard source was used for energy and detection efficiency calibration. The energy resolution was measured to be 2.6 keV for the 1.3-MeV  $\gamma$  ray transition in  $^{60}\text{Co}$ . In the measurement of  $\gamma$  rays, the add-back mode can be used to improve the photopeak efficiency and the signal-to-background ratio. The total photopeak efficiencies with and without the add-back mode were 1.4 and 1.0%, respectively, for 1-MeV  $\gamma$  rays.

We also detected  $\beta$  rays from the implanted nuclei for the identification of  $\beta$ - $\gamma$  coincidence events and improvement of the signal-to-background ratio in the  $\gamma$ -ray energy spectra. The  $\beta$  rays were detected with two sets of  $\Delta E$ - $\Delta E$ - $E$  plastic scintillator telescopes [10], placed above and below the stopper. The dimensions of each  $\Delta E$  counter was 200 × 200 × 2 mm<sup>3</sup>. The  $\Delta E$  detectors were placed 8.3 cm from the stopper, covering 42% of the solid angle. Each  $\Delta E$  detector had two photomultiplier tubes at either end, and a logical AND of signals from both tubes defined the detection of a  $\beta$  ray. The average of the timing signals from the two photomultiplier tubes provided the detection time. Each  $E$  counter had a cylindrical shape with a diameter of 240 mm and a height of 130 mm. The thickness of these detectors allowed a measurement of  $\beta$ -ray energies up to about 30 MeV.

The data acquisition system was triggered by a  $\beta$  hit event, a single  $\gamma$  hit event, a  $\beta$ - $\gamma$  coincidence event, or a  $\gamma$ - $\gamma$  (clover-clover) coincidence event. A  $\beta$  hit event was defined by a logical OR of signals from the first layer  $\Delta E$  counters of the  $\beta$ -ray telescopes. A  $\gamma$  hit event was defined by a signal from a Ge detector. A  $\gamma$ - $\gamma$  coincidence was not a coincidence between individual clover Ge crystals but among the clover Ge detectors. To suppress the trigger rate for single  $\gamma$  events, the threshold level was set at 600 keV. For  $\beta$ - $\gamma$  and  $\gamma$ - $\gamma$  events, the threshold was set at a lower 100 keV.  $\beta$ - $\gamma$  coincidence events were used for identifying  $\beta$ -delayed  $\gamma$  rays, and  $\gamma$ - $\gamma$  coincidence events were used for observing cascade decays.

To obtain decay curves, the time of each event as measured from the start of the beam-on period was recorded. The shape of the decay curves could be distorted by the rate dependence of the dead time in the data acquisition system. Thus, random pulses were mixed with the triggers so that the dead-time spectrum could be deduced and used to correct the distortion in the decay curves.

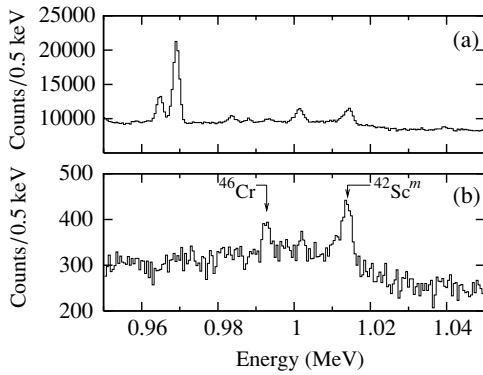


FIG. 2.  $\gamma$ -ray energy spectra around 993 keV in add-back mode (a) without  $\beta$  coincidence and (b) with  $\beta$  coincidence.

### III. DATA ANALYSIS AND RESULTS

We observed the 993-keV  $\gamma$  rays from the GT decay of  $^{46}\text{Cr}$  and determined the branching ratio of this decay and the half-life of  $^{46}\text{Cr}$ . From these values,  $B(\text{GT})$  was deduced. The Fermi transition strength to the g.s. of  $^{46}\text{V}$  was compared to the theoretical value so as to check the reliability of the experimental results. In this section, we describe the details of the data analysis and the results of the experiment.

#### A. Observation of the 993-keV peak

To identify the 993-keV  $\gamma$  rays originating from  $\beta$  emitters, we compared two  $\gamma$ -ray energy spectra, namely a  $\gamma$  single spectrum and a  $\beta$ - $\gamma$  coincidence spectrum, as shown in Figs. 2(a) and 2(b), respectively. A peak at 993 keV was observed in both spectra, thus confirming that 993-keV  $\gamma$  rays are associated with a  $\beta$ -delayed transition. The observed energy of these  $\gamma$  rays is  $993.1 \pm 0.2$  keV, which agrees with the energy of 993.2 keV of the known first  $1^+$  excited state of  $^{46}\text{V}$  [4].

Note that there is no known  $\gamma$  transition in the vicinity of this peak that is associated with the  $\beta$  decay of beam contaminants. Figure 3 shows the  $\gamma$ -ray energy spectra in an energy range up to 1.6 MeV, observed in the  $\beta$ - $\gamma$  coincidence measurement. The strong  $\gamma$  lines at 437, 1228, and 1525 keV are  $\beta$ -delayed  $\gamma$  rays of  $^{42}\text{Sc}^m$ , a contaminant in the  $^{46}\text{Cr}$  beam. The line at 1014 keV in Fig. 2(b) also originates from  $^{42}\text{Sc}^m$ ; this is

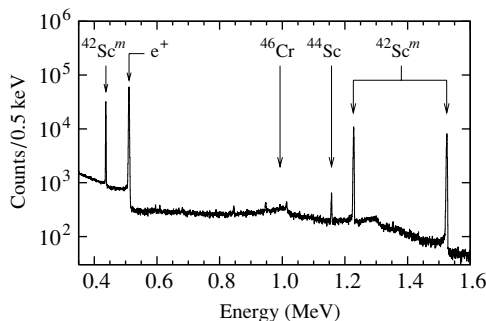


FIG. 3.  $\gamma$ -ray energy spectra in add-back mode with  $\beta$  coincidence.

a single escape peak of the 1525-keV  $\gamma$  rays. The peak at 1157 keV comes from the  $\beta$  decay of  $^{44}\text{Sc}$ .

Another way to check the origin of the 993-keV  $\gamma$  rays is to examine their time structure. The half-life of the source of these  $\gamma$  rays agrees with the half-life of  $^{46}\text{Cr}$  given in the literature [3], as will be shown later. From the above facts, we conclude that these  $\gamma$  rays depopulate the  $1_1^+$  state in  $^{46}\text{V}$  fed by the GT decay of the ground state of  $^{46}\text{Cr}$ .

#### B. Branching ratios

The branching ratio of the GT transition to the  $1_1^+$  state in  $^{46}\text{V}$  is determined from the  $\gamma$ -ray spectrum. The obtained value was  $b_{\text{GT}} = 0.216 \pm 0.050$ . This value is given by

$$b_{\text{GT}} = \frac{N_\gamma}{\epsilon_\gamma \times d \times N_i}, \quad (1)$$

where  $N_\gamma$  is the number of counts in the 993-keV peak after background subtraction,  $d$  is the dead-time correction, and  $N_i$  is the number of implanted  $^{46}\text{Cr}$  nuclei. In the following, we describe how we determined  $N_i$  and  $N_\gamma$ .

The number of implanted  $^{46}\text{Cr}$  fragments was determined from the total number of implanted ions and the ratio of  $^{46}\text{Cr}$  to the total number of implanted ions, as described above. Figure 4 shows a TOF spectrum of the ions implanted in the stopper. The ratio of  $^{46}\text{Cr}$  was determined to be  $(7.09 \pm 0.44) \times 10^{-4}$  from this spectrum. In determining the ratio, the purity of  $^{46}\text{Cr}$  in the TOF range of  $^{46}\text{Cr}$  was taken into account because we could not separate  $^{44}\text{V}$  from  $^{46}\text{Cr}$  from only the TOF information. The purity was estimated to be 93% from the  $\Delta E$ -TOF information. The error of the ratio of  $^{46}\text{Cr}$  to the total number of implanted ions includes systematic errors. One of the major sources of error is the uncertainty in the transmission efficiency from F2 to the stopper, originating from the difference in efficiency for  $^{46}\text{Cr}$  and  $^{44}\text{V}$ , both selected in the TOF gate. The uncertainty was estimated to be 4.8% using the beam profile information obtained by the F3PPACs. The total number of implanted ions was  $1.23 \times 10^9$ . From this number and the ratio of  $^{46}\text{Cr}$  to the total number of implanted ions, the number of implanted  $^{46}\text{Cr}$  was determined to be  $(8.75 \pm 0.54) \times 10^5$ .

To determine  $N_\gamma$ , we analyzed the  $\gamma$ -ray energy spectrum obtained from the  $\gamma$  single triggered events. The identification

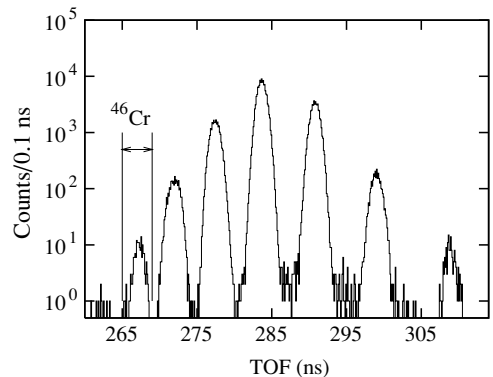


FIG. 4. TOF spectrum of ions implanted in stopper.

of  $\gamma$  single events enabled us to avoid the additional uncertainty in the  $\beta$  detection efficiency. In this analysis, we did not use the add-back mode because of the relatively high energy-threshold level for the single event trigger. The number of 993-keV  $\gamma$  rays was obtained by a Gaussian fit of the peak; the obtained  $\gamma$ -ray yield was  $1949 \pm 403$ . The error in this value is statistical. The contribution from  $\gamma$  rays from  $^{46}\text{Cr}$  stopped at the collimator had to be subtracted from this value. We determined the detection efficiency of  $\gamma$  rays from the collimator by using  $\gamma$  rays from  $^{42}\text{Sc}$ . The number of observed  $\gamma$  rays from the stopper should be the same in each Ge crystal, but in practice the number of observed  $\gamma$  rays coming from the collimator is not the same, because the distance and the amount of absorbing matter between the collimator and each Ge crystal is different. Thus we can estimate the number of  $\gamma$  rays from the collimator from the difference in the number of observed  $\gamma$  rays at each crystal and thereby determine the detection efficiency of  $\gamma$  rays from the collimator. Finally, the number of 993-keV  $\gamma$  rays was found to be  $1455 \pm 322$ .

The branching ratio of the GT transition to the  $1_1^+$  state in  $^{46}\text{V}$  was determined to be  $b_{\text{GT}} = 0.216 \pm 0.050$ . If we assume that only the  $1_1^+$  state is populated by a GT transition, the branching ratio for the Fermi transition to the g.s. is  $b_F = 0.784 \pm 0.050$ . This number represents only an upper limit, because there may be GT transitions to higher lying  $1^+, T = 0$  states. The assumption made in Ref. [11] that  $\gamma$  transitions from any higher states populated by GT transitions will ultimately populate the  $1_1^+$  state should be taken with caution. The  $1^+, T = 0$  states usually decay mainly to the  $0^+, T = 1$  g.s. through an isovector transition with a large  $B(M1)$  [12].

### C. Decay curve

To obtain a decay curve, we used the  $\gamma$ -ray energy spectrum in add-back mode with  $\beta$  coincidence, which provided us with a better peak-to-background ratio. The decay curve for events in coincidence with 990.5–994.5-keV  $\gamma$  rays is shown in Fig. 5. The half-life of  $^{46}\text{Cr}$  was obtained by fitting a function

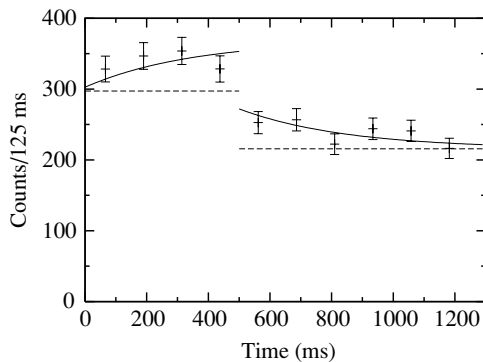


FIG. 5. Decay curve obtained in coincidence with 993-keV  $\gamma$  rays. The curve shows a fit to a decay plus a constant background. The background is shown by the dotted line. The periods of 0–500 ms and 500–1290 ms correspond to the beam-on and beam-off periods, respectively.

to the decay curve, with the dead-time correction and the background of the decay curve considered. The obtained value of the half-life was  $240 \pm 140$  ms. This value is consistent with the previous data  $T_{1/2} = 260 \pm 60$  ms [3]. The details of the fitting procedure are given in the Appendix.

### D. Gamow-Teller transition strength

The next step is the calculation of the reduced half-life  $ft$ . As mentioned above, the half-life of  $^{46}\text{Cr}$  measured in this experiment and the value given in Ref. [3] are statistically consistent. Therefore, we use the weighted average of these two values,  $T_{1/2} = 0.257 \pm 0.055$  s. Hence, the partial half-life of the GT transition is  $t = 1.190 \pm 0.375$  s.

To calculate the statistical function  $f$ , we must know the difference of the atomic masses of the parent and daughter nuclei. The mass excess of  $^{46}\text{Cr}$  has been experimentally determined [3,13]. We adopt the value  $D(^{46}\text{Cr}) = -29.471 \pm 0.020$  MeV [14], where  $D$  denotes the mass excess. The value  $D(^{46}\text{V}) = -37.070739 \pm 0.0015$  MeV was taken from the same source. We obtained an atomic mass difference between the ground states of the two nuclei of  $Q_\beta = 7.6029 \pm 0.02$  MeV.

The  $f$  functions were calculated using a BNL code [15] and checked against Wilkinson's table [16]. The value of the  $f$  function for the decay to the 0.993-MeV state in  $^{46}\text{V}$  was  $f = 5000$ . This gives  $ft = 5950 \pm 1875$  s. The GT strength is defined as

$$B(\text{GT}; I_i^\pi, T_i, T_{zi} \rightarrow I_f^\pi, T_f, T_{zf}) = \frac{1}{2I_i + 1} \left\langle I_f, T_f, T_{zf} \left\| \sum_k \sigma^k t_-^k \right\| I_i, T_i, T_{zi} \right\rangle^2, \quad (2)$$

with  $t_- = \frac{1}{2}(\tau_1 - i\tau_2)$  [17]. The summation is carried out over the nucleons participating in the  $\beta$  decay. The relation between  $ft$  and  $B(\text{GT})$  [17] is

$$B(\text{GT}) = \frac{K}{(g_A/g_V)^2 ft}, \quad (3)$$

with  $K = 6145$  s and  $g_A/g_V = -1.266$  [18]. From this we obtain  $B(\text{GT}) = 0.64 \pm 0.20$ .

### E. Fermi transition strength

It is also interesting to examine the Fermi transition to the g.s. of  $^{46}\text{V}$ . As shown above,  $b_F = 0.784 \pm 0.050$ . This corresponds to a Fermi partial half-life of  $t_F = 0.328$  s. The statistical function has the values  $f = 10\,715$  and  $ft_F = 3540 \pm 789$ . From these, we can calculate the Fermi strength by a formula analog to Eq. (3),  $B(F) = 1.74 \pm 0.38$ , which is statistically consistent with the simple theoretical value  $B(F) = 2$ . The latter does not include radiative and charge-dependent corrections [11,18], which are at the 1% level.

#### IV. DISCUSSION

In this section, we discuss the obtained  $B(\text{GT})$  value from two viewpoints. First, we compared the obtained value with the values of neighboring nuclei and found that the  $B(\text{GT})$  value of  $^{46}\text{Cr}$  is similar to those of neighboring nuclei. We also made a comparison with theoretical calculations with the shell model and the quasideuteron model [7]. We found that the shell model calculation using the FPD6 interaction [19] (see below) was in good agreement with the measured value.

##### A. Comparison with neighboring nuclei

Values for similar transitions to the  $1_1^+$  state in neighboring nuclei are  $B(\text{GT}) = 0.59 \pm 0.15$  in the decay of  $^{50}\text{Fe}$  [11] and  $B(\text{GT}) = 0.68 \pm 0.15$  in the decay of  $^{54}\text{Ni}$  [20]. One should take into account the fact that  $^{50}\text{Fe}$  as well as  $^{46}\text{Cr}$  are probably deformed or, at least, have collective features [7]. Interaction with a deformed mean field leads to fragmentation of the  $1^+$  state and of the GT strength (see Sec. IV B). Therefore, in this case we may expect some GT strength going to higher  $1^+$  bound states.

##### B. Comparison with theory

At present, the most reliable way to calculate GT strength is by the shell model. GT strength is distributed over a wide range of excitation energies (which also include unbound states). A correct quantitative evaluation should take into account particle-hole excitations to higher shells, starting from  $2\hbar\omega$  [21] and perhaps other degrees of freedom [22]. Such calculations have been done so far only for light nuclei in the  $1p$  shell, e.g., in Ref. [23]. Even in the  $A = 40$  region, the best one can do is to carry out calculations in the full  $pf$  model space. The truncation of the model space unavoidably leads to overestimation. This is the main reason why an empirical quenching factor is required to bring the theoretical and experimental values into agreement.

The excitation energies and electromagnetic transition strengths for  $^{46}\text{V}$  have been calculated in the full shell model  $pf$  space [4]. In the present work, this calculation has been extended to GT matrix elements. The following two-body interactions have been used:

- (1) The KB3 interaction, which is based on the Kuo-Brown  $G$  matrix [24], with modified monopole parts [25]. In the present calculation, we replaced this interaction by the improved version KB3G [26].
- (2) The FPD6 interaction, whose matrix elements are calculated using one-boson-exchange-potential-type functions [19]; the parameters have been adapted to the  $pf$  region.
- (3) The GXPF2 interaction [27], which is an effective interaction devised for use in the full  $pf$  shell space.

A calculation with the phenomenological quasideuteron (QD) model [7] was also done. In this model, two nucleons occupying the same single-particle state are coupled to an even-even  $Z = N$  core with  $T = 0$ . If the nuclear potential is spherically symmetric, the model does not explicitly contain a

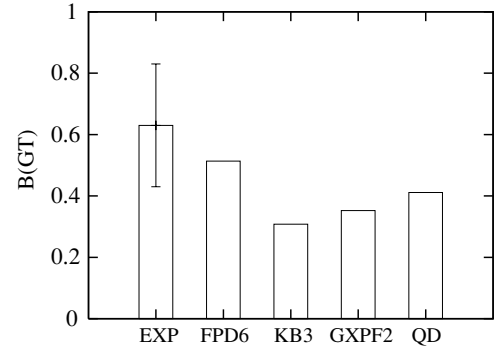


FIG. 6. Comparison between experimental (EXP) and quenched theoretical values of  $B(\text{GT}; 0^+ \rightarrow 1_1^+)$ . The calculated  $B(\text{GT})$  values are quenched by a factor of 0.55.

two-body interaction between valence nucleons. In the case of  $^{46}\text{V}$ , a deformed core with an effective deformation of  $\beta = 0.27$  was used, and the two nucleons were considered to occupy Nilsson orbitals. In this way, a two-body interaction is implicitly contained in the deformed mean field. As mentioned above, interaction with the mean field leads to fragmentation of the spherical states; so far, only the  $1_1^+$  state in  $^{46}\text{V}$  has been populated both in fusion reactions [4] and in the present experiment. Of course, the GT strength is fragmented also.

It is worth considering what happens in a hypothetical spherical nucleus. To get at least a qualitative idea, we carried out a shell model calculation without two-body interactions and assumed that the valence nucleons had the configurations  $|\pi f_{7/2}^4(\nu f_{7/2})^2; 0^+\rangle$  and  $|\pi f_{7/2}^3(\nu f_{7/2})^3; 1^+\rangle$  in  $^{46}\text{Cr}$  and  $^{46}\text{V}$ , respectively. We obtained seven degenerate lowest  $1^+$  states, each of them having the same GT strength  $B(\text{GT}) = 0.42$ . If we switched on a residual interaction, the degeneracy was lifted and the distribution of GT strength over the first seven  $1^+$  states was no longer uniform. This simple example also shows the crucial role played by the two-body interaction in the GT decay strength.

The values of  $B(\text{GT}; 0^+, T = 1 \rightarrow 1_1^+, T = 0)$  calculated with the shell model, as well as with the QD model, are shown in Fig. 6. The most plausible theoretical value is that obtained by using the FPD6 interaction. It is usually assumed that the GT matrix element calculated in the full  $pf$  shell needs a quenching factor of 0.74. This means that the value of the calculated  $B(\text{GT})$  must be quenched by a factor of 0.55. The value calculated for the FPD6 interaction and quenched by this factor, namely  $B(\text{GT}) = 0.51$ , is in reasonable agreement with the measured  $B(\text{GT}) = 0.64 \pm 0.20$ . However, the large standard deviation does not allow a detailed comparison with theory.

#### V. CONCLUSION

The Gamow-Teller decay of  $^{46}\text{Cr}$  to the  $1^+, T = 0$  state of  $^{46}\text{V}$  has been observed for the first time. A  $^{46}\text{Cr}$  secondary beam was produced by the fragmentation of a primary  $^{50}\text{Cr}$  beam and was identified after magnetic separation by measuring the time of flight and the energy loss in a solid state detector. The secondary beam was stopped in a

plastic scintillator. The  $\gamma$  rays following the GT decay were observed by measuring single- $\gamma$  spectra with four clover Ge detectors, as well as coincidences with two  $\beta$ -scintillator telescopes. This shows again that the fragmentation reaction, followed by  $\beta$ - $\gamma$ -ray spectroscopy on the stopped beam, constitutes a powerful tool for the investigation of unstable nuclei.

As expected, the GT decay of the  $T = 1$   $^{46}\text{Cr}$  nucleus to a  $I^\pi = 1^+, T = 0$  state of the odd-odd  $N = Z$   $^{46}\text{V}$  nucleus was observed. The branching ratio to the  $1_1^+$  state was  $0.216 \pm 0.050$ . This GT decay has a relatively large value of GT strength of  $B(\text{GT}) = 0.64 \pm 0.20$ . Similar values have been observed in the GT decay of neighboring nuclei. Since previous investigations show that both the parent and daughter nuclei are deformed or at least have collective properties, the  $1^+$  state of  $^{46}\text{V}$  populated in this experiment is only the lowest among several  $1^+$  states located inside the  $\beta$  energy window. Therefore, the observed  $B(\text{GT})$  represents only a fragment of the total GT strength.

This experimental GT strength was compared with shell model calculations in the full  $pf$  space, as well as with calculations done with the phenomenological quasideuteron model. The shell model calculation using the FPD6 two-body interaction gives a value closest to the experimental result. This theoretical value, reduced by the standard quenching factor, is in reasonable agreement with the measured value.

Since accurate measurements of favored-allowed GT transitions are important because of their high sensitivity to the interactions used in the shell model, an investigation

of the GT decay of  $^{46}\text{Cr}$  with higher statistics is certainly desirable.

#### ACKNOWLEDGMENTS

The authors would like to thank Prof. A. Arima, Prof. A. Brown, Prof. H. Ejiri, Prof. F. Iachello, Prof. Y. Fujita, Prof. A. Poves, and Prof. I. Talmi for stimulating discussions and suggestions.

#### APPENDIX

We here describe the method of obtaining the half-life of  $^{46}\text{Cr}$ , which involves fitting a function to the decay curve. The dead time and background must be taken into account in this fitting.

The decay curve of  $^{46}\text{Cr}$  was distorted by the dead time, which was time dependent. For the dead-time correction, we used a random trigger. The time structure of the random trigger shows how the observed decay curve was distorted by the dead time, allowing the observed decay curve to be corrected by this random trigger.

We assumed that the energy dependence of the time structure of the background around 993 keV was smooth because the background of the decay curve mainly consisted of Compton-scattered  $\gamma$  rays. The time structures of the 986.5–990.5 and 994.5–998.5-keV windows of the  $\gamma$ -ray energy spectrum were used for estimating the background.

A fit to a function for the decay curve uses

$$N(t) = \begin{cases} AB\tau I \exp(-\frac{t}{\tau}) + Ia + c_{\text{on}} & (0 \leq t \leq 500 \text{ ms}) \\ (A \exp(-\frac{500}{\tau}) + 1)\tau IB \exp(-\frac{t-500}{\tau}) + c_{\text{off}} & (500 \leq t \leq 1290 \text{ ms}), \end{cases} \quad (\text{A1})$$

$$A \equiv \frac{\exp(-\frac{790}{\tau}) - 1}{1 - \exp(-\frac{1290}{\tau})}, \quad (\text{A2})$$

$$B \equiv 1 - \exp(-\frac{a}{\tau}), \quad (\text{A3})$$

where  $I$ ,  $\tau$ ,  $c_{\text{on}}$ , and  $c_{\text{off}}$  are free parameters and  $a = 10$  ms is the bin width;  $\tau$  corresponds to the life-time of  $^{46}\text{Cr}$ , and  $c_{\text{on}}$

and  $c_{\text{off}}$  correspond to the background. For the background, the functional form is

$$N(t) = \begin{cases} c_{\text{on}} & (0 \leq t \leq 500 \text{ ms}) \\ c_{\text{off}} & (500 \leq t \leq 1290 \text{ ms}), \end{cases} \quad (\text{A4})$$

The maximum likelihood method was used to fit the three spectra, namely, the decay curves of the peak and the two backgrounds.

- [1] P. Van Isacker, Rep. Prog. Phys. **69**, 1661 (1999).
- [2] I. Talmi, *Simple Models of Complex Nuclei* (Harwood Academic, Chur, Switzerland, 1993).
- [3] J. Zioni *et al.*, Nucl. Phys. **A181**, 465 (1972).
- [4] C. Friessner, N. Pietralla, A. Schmidt, I. Schneider, Y. Utsuno, T. Otsuka, and P. von Brentano, Phys. Rev. C **60**, 011304(R) (1999).
- [5] S. M. Lenzi *et al.*, Phys. Rev. C **60**, 021303(R) (1999).

- [6] C. D. O'Leary *et al.*, Phys. Lett. **B459**, 73 (1999).
- [7] A. F. Lisetskiy, R. V. Jolos, N. Pietralla, and P. von Brentano, Phys. Rev. C **60**, 064310 (1999); A. F. Lisetskiy *et al.*, Phys. Lett. **B512**, 512 (2001).
- [8] T. Kubo *et al.*, Nucl. Instrum. Methods B **70**, 309 (1992).
- [9] J. A. Winger *et al.*, Nucl. Instrum. Methods B **70**, 380 (1992).
- [10] N. Aoi *et al.*, Phys. Rev. C **66**, 014301 (2002).
- [11] V. T. Koslowsky *et al.*, Nucl. Phys. **A624**, 293 (1997).

- [12] P. von Brentano *et al.*, Nucl. Phys. **A704**, 115c (2002).
- [13] V. Borrel *et al.*, Z. Phys. A **344**, 135 (1992).
- [14] G. Audi *et al.*, Nucl. Phys. **A624**, 1 (1997).
- [15] ENSDF Analysis programs (<http://www.nndc.bnl.gov/index.jsp>).
- [16] D. H. Wilkinson and B. E. F. Macefield, Nucl. Phys. **A232**, 58 (1974).
- [17] L. Zamick and D. C. Zheng, Phys. Rev. C **37**, 1675 (1987).
- [18] K. Schreckenbach *et al.*, Phys. Lett. **B349**, 427 (1995).
- [19] W. A. Richter *et al.*, Nucl. Phys. **A253**, 325 (1991).
- [20] I. Reusen *et al.*, Phys. Rev. C **59**, 2416 (1999).
- [21] A. Arima *et al.*, Adv. Nucl. Phys. (Plenum, New York, 1987), Vol. 18.
- [22] F. Osterfeld *et al.*, Rev. Mod. Phys. **64**, 491 (1992).
- [23] T. Suzuki, R. Fujimoto, and T. Otsuka, Phys. Rev. C **67**, 044302 (2003).
- [24] T. T. S. Kuo and G. E. Brown, Nucl. Phys. **A114**, 241 (1968).
- [25] A. Poves and A. Zuker, Phys. Rep. **70**, 235 (1981).
- [26] A. Poves *et al.*, Nucl. Phys. **A694**, 157 (2001).
- [27] M. Honma, T. Otsuka, B. A. Brown, and T. Mizusaki, Phys. Rev. C **65**, 061301(R) (2002).